CHAPTER 7

GROWTH OF Sb_2Te_3 AND Sb_2Te_3 BASED CRYSTALS

The crystal growth technique for the preparation of a useful thermoelectric material involves two distinct processes: first, the selection and reaction of component elements to form the compound or alloy and second, the determination of the crystal growth conditions under which the best possible thermoelectric properties of a particular compound or alloy may be achieved. Considering the main practical factors concerning the materials, viz; a) volatility or dissociability b) chemical reactivity and c) the melting point, it has been found that the best p-type materials for use in room temperature thermoelectric devices are made of solid solutions formed by Bi_2Te_3 or Sb_2Te_3 compounds. It is known that the efficiency of these materials depends on the preparation method.

There have been various reports of crystal growth of this family of materials. Abrikosov et al.[1,2] have obtained single crystals of Sb_2Te_3 and the $Bi_{0.5}Sb_{1.5}Te_3$ solid solution with a perfect structure, oriented in different crystallographic directions by the Czochralski method of pulling from a melt with liquid-phase makeup from a floating crucible. Berkholtz[3] investigated properties of single crystals of the Bi_2Te_3–Sb_2Te_3 alloys which had been grown in a Bridgman furnace at a rate of 1 mm/min and reported a maximum of mobility values near 33.3 mole% Sb_2Te_3 and a minimum in these values near 66.7 mole % Sb_2Te_3. Testardi and Wiese[4], in a study of the densities of zone-leveled crystals and of quenched ingots, find a gentle peaking of densities at compositions in the vicinity of 33.3 and 66.7 mole % Sb_2Te_3 for the zone leveled material, but not for the quenched material. Cosgrove et al.[5] report that as the growth rate increases for $BiSbTe_3$ doped with 0.56 wt % Se and grown using the Bridgman technique, the Seebeck effect decreases and the lattice thermal conductivity increases. These effects are primarily attributed to the variation in the degree of microsegregation

produced in the crystals as a function of freezing conditions. Wiese and Pyle[6] report that the pseudo binary phase diagram of the Bi_2Te_3–Sb_2Te_3 system is of the solid-solution type, where the liquidus and solidus curves across the system are nearly congruent. However, Rosi et al.[7] find a change in the sign of the distribution coefficient k in the interior of the phase diagram for materials grown at a rate of 6 mm/h and attribute this phenomenon to a minimum in the solid solubility curve in the vicinity of 30% Sb_2Te_3. Yasuda et al.[8] have studied the effect of magnetic field on macrosegregation in unidirectionally solidified $(BiSb)_2Te_3$. F. Koenig[9] have grown $Bi_{0.5}Sb_{1.5}Te_3$ crystals by zone melting under microgravity. Ivanova et al.[10,11] have assessed the inhomogeneity of Czochralski-grown crystals of Bi_2Te_3-Sb_2Te_3 solid solutions by measuring the longitudinal and cross-sectional distributions of thermoelectric power. The most non-uniform cross-sectional distributions of thermoelectric power were observed at the ends of the crystal. Thermoelectric properties are found to depend substantially on growth conditions[10]. A decrease in longitudinal inhomogeneity was provided by varying the pulling rate during growth. It was shown[11] that heat treatment of samples cut from various parts of the crystal can reduce radial inhomogeneity. They have also studied the homogeneity of $Bi_{0.5}Sb_{1.5}Te_3$ single crystals[12] grown at various rotation rates of the crucible and the ingot. As the crucible rotation rate is increased from 6 to 15 rpm, the spread in thermopower over the crystal slice is reduced by half. The change in the ingot rotation rate from 20 to 40 rpm has a weaker effect on crystal homogeneity. It has been reported that high quality single crystals grown by Traveling Heater Method (T. H. M) with higher thermoelectric efficiency could be achieved in the case of Bismuth telluride[13] and Antimony telluride[14]. Caillat et al.[15] have studied the thermoelectric properties of $(Bi_xSb_{1-x})_2Te_3$ single crystal solid solutions grown by the T. H. M. method and determined a maximum in the figure of merit $Z = 3.2 \times 10^{-3}\ ^{\circ}K^{-1}$ for the solid solution with a composition $Bi_9Sb_{31}Te_{60}$. Rosenberg and Strauss[16] have studied

the structural and thermoelectric properties of the solid solutions of In_2Te_3 in Sb_2Te_3 and Bi_2Te_3 formed by directional freezing.

Bismuth telluride based alloys have been exclusively prepared by the conventional melt technique followed occasionally by the conventional sintering technique[15,17,18,19]. The properties of bismuth telluride based alloys prepared by the PIES method (Pulverised and Intermixed Elements Sintering method) are quite different from the alloys prepared by the conventional techniques. The PIES method has been investigated as a new preparation technique not only for bismuth telluride based alloys [20,21,22] but also for silicon-germanium based alloys [23], rare earth sulfides[24] and so on. It has a number of advantages over the conventional technique: for example, low energy inventory for preparation, low cost and short processing period, a potential for reducing grain size which favors a reduction in the thermal conductivity and an enhancement in the mechanical strength. The thermoelectric figure of merit of $(Bi_2Te_3)_{0.2}(Sb_2Te_3)_{0.8}$ based PIES material was reported[25] to be comparable to that of the conventional material. However it has not been possible to obtain results which would precisely match with those with the best single crystal.

The discussion that follows deals with the experimental techniques employed in the present work for synthesizing, crystal growth and microtopographic study of the Sb_2Te_3 and Sb_2Te_3 based single crystals and the results obtained thereby. The crystals were grown from melt by zone melting[26] and Bridgman[27] techniques. For surface observations, optical microscopy and scanning electron microscopy (SEM) were used.

SYNTHESIZING THE ALLOY

In order to grow homogeneous single crystals of $Bi_xSb_{2-x}Te_3$ (x = 0, 0.2, 0.5, 1) and $In_{0.2}Sb_{1.8}Te_3$ by the Bridgman and zone-melting methods, it is necessary to start with a relatively homogeneous solid charge. Growing homogeneous ingots with well-controlled composition depends on the knowledge of the phase diagram. Fig. 1, 2, and 3 show the phase diagrams of the Sb_2Te_3[28],

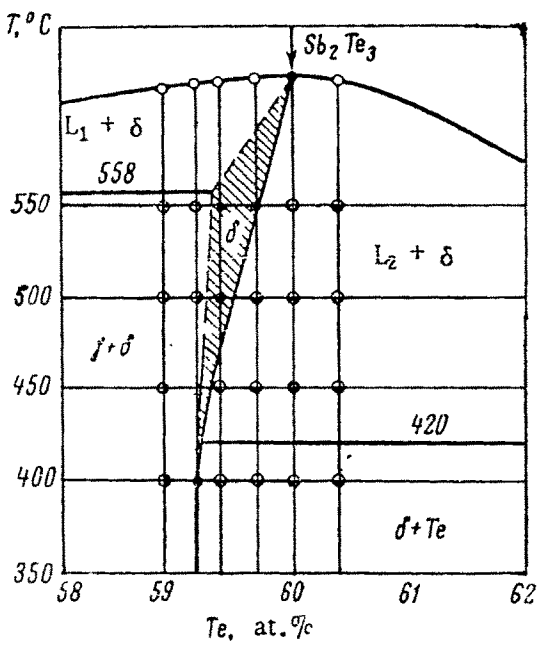

Fig. 1. Phase diagram of the Sb-Te system in the region of the compound Sb_2Te_3

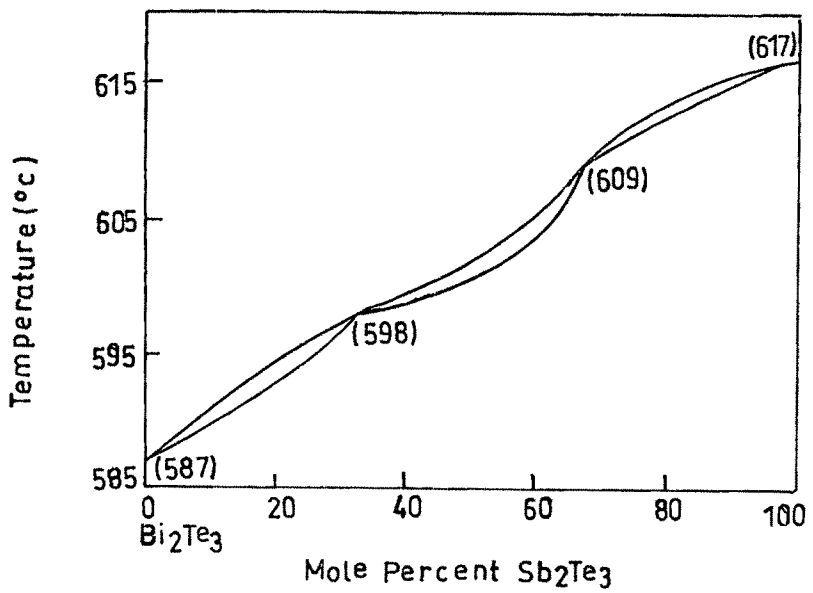

Fig. 2. Bi_2Te_3-Sb_2Te_3 pseudo-binary phase diagram

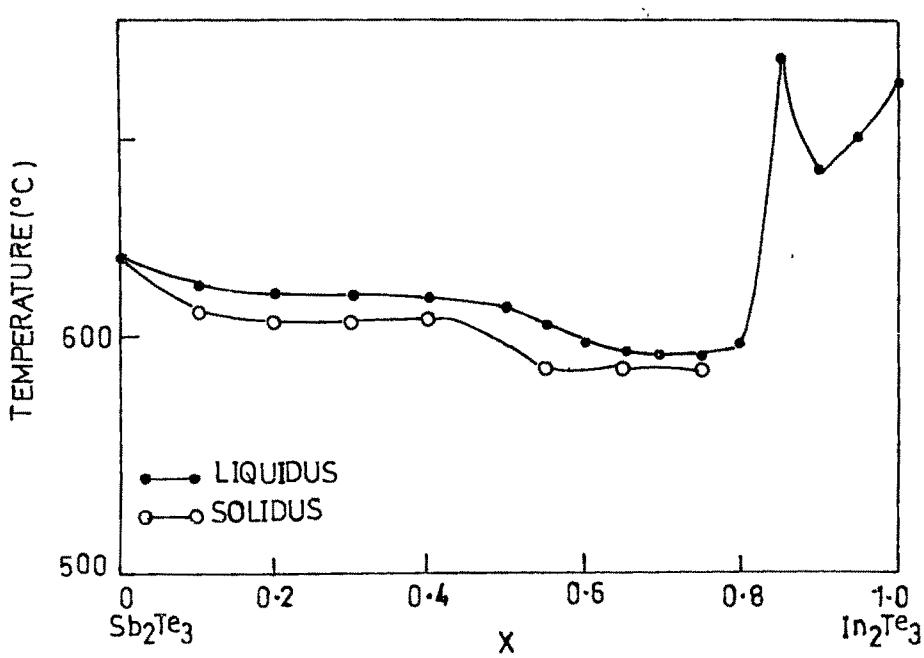

Fig. 3. Phase diagram of the Sb_2Te_3-In_2Te_3 pseudobinary system

Bi_2Te_3-Sb_2Te_3[29], In_2Te_3-Sb_2Te_3[16] systems, respectively. Earlier investigations[30] have established the existence of one chemical compound, viz., Sb_2Te_3, in the Sb-Te system. This compound forms eutectics with antimony and tellurium. The phase diagram of the Sb-Te [28] system in the region of Sb_2Te_3 shows that Sb_2Te_3 exists in the stoichiometric form only at temperatures close to the liquidus curve. When the temperature is lowered, a partial retrograde melting is observed and a tellurium-rich liquid is obtained. The composition of the δ phase shifts in the direction of excess antimony, reaching its largest degree of departure from stoichiometry at 59.2 at. % Te at 400^0C. The stoichiometric alloy if quenched from temperatures below the liquidus curve, there results, in addition to the δ phase, a small amount of δ + Te eutectic. The departure of Sb_2Te_3 from stoichiometry has been confirmed by Offergeld and Cakenberghe[31]. The phase diagram of Bi_2Te_3-Sb_2Te_3[29] shows that the pseudo-binary system is of the solid solution type and that there is only a small separation between the liquidus and solidus curves, which makes the solute distribution coefficient nearly equal to one. The phase diagram of In_2Te_3-Sb_2Te_3[16] shows that the layered hexagonal structure of the mixed crystals is retained for In concentrations upto x = 0.4.

In order to ensure a uniform charge for crystal growth, an alloy mixing unit was used and it is described below.

The apparatus consists of a cylindrical resistance furnace prepared in the usual way and properly lagged so as to avoid radiation losses. Along the axis of the furnace is supported a quartz tube (60 cm in length) of 3.0 cm in diameter. The two ends of the quartz tube are fitted to two brass sockets at both the ends in which the tube can be easily clamped. The sockets are pivoted on frictionless bearings and the axis adjusted so as to have a smooth motion without wobbling, with the help of two stout supports at the two ends. The brass socket at one end of the tube is connected to a small electric motor. The whole apparatus is fitted on a heavy wooden base. The photograph of the unit is shown in Fig. 4.

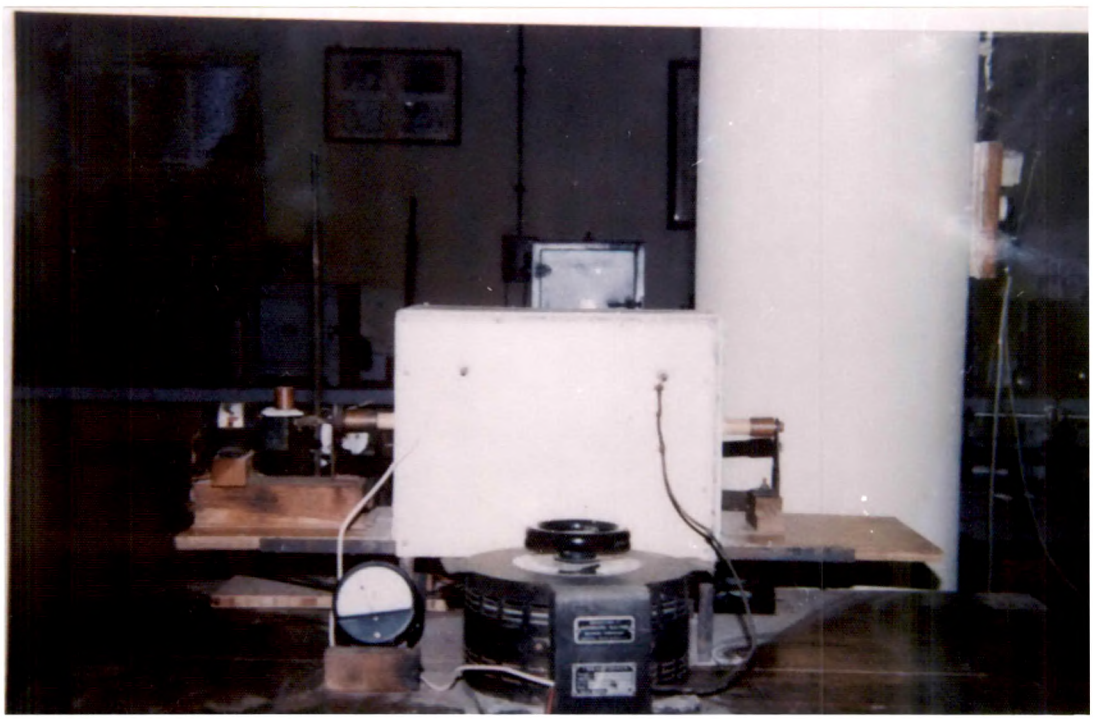

Fig. 4. Alloy Mixing Unit

The elements used, viz., antimony, bismuth, tellurium and indium were each of 5N purity purchased from either Koch Light Laboratories, England or Nuclear Fuel Complex, Hyderabad. The stoichiometric proportions of all the components were weighed accurately upto 10 microgram using a semimicrobalance and filled in a quartz ampoule of about 10 cm length and 1 cm diameter. The quartz tube was then sealed under a vacuum of ~ 2×10^{-5} Torr. The ampoule was placed in the uniform temperature zone of about 15 cm length inside the quartz tube of the horizontal furnace and was kept static for about a day. The temperature was kept about 75°C above the melting point of the alloy, i.e., at 700°C. Then the quartz tube was rotated at one r.p.m. by a motor attached to one of its ends. The rotation of the quartz tube gives rocking movement to the ampoule and stirs the molten charge. Usually, ten rotations followed by an idle run of one-day is found sufficient. After this, the molten charge is slowly cooled. This procedure produces fairly homogeneous alloys of $Bi_xSb_{2-x}Te_3$ (x = 0, 0.2, 0.5, 1), and $In_{0.2}Sb_{1.8}Te_3$.

CRYSTAL GROWTH

For crystal growth of $Bi_xSb_{2-x}Te_3$ (x = 0, 0.2, 0.5, 1), and $In_{0.2}Sb_{1.8}Te_3$ by the Bridgman technique, the ampoule with the ingot was kept in the vertical Bridgman furnace (Fig. 5). The length of the core of the furnace is about 45 cm. The temperature profile of the furnace is shown in Fig. 6. The ampoule was kept steady for 24 hours in the upper hot zone of the furnace and then lowered into the cold zone at a rate of 0.35 cm/hr and through a temperature gradient of about 35°C/cm. The crystals obtained were about 4 cm in length and 1 cm in diameter. They could be cleaved easily. Microscopically the cleavage plane of the crystal was found to be fairly planar. These crystals have (111) cleavage.

The single crystals of $Bi_xSb_{2-x}Te_{3-x}$ (x = 0, 0.2, 0.5, 1) were prepared using the zone melting method also (Fig 7). The temperature profile of the zone furnace is shown in Fig. 8. The starting ingot was synthesized as mentioned above and then to level off impurities, 5 passes in alternate directions were given and finally

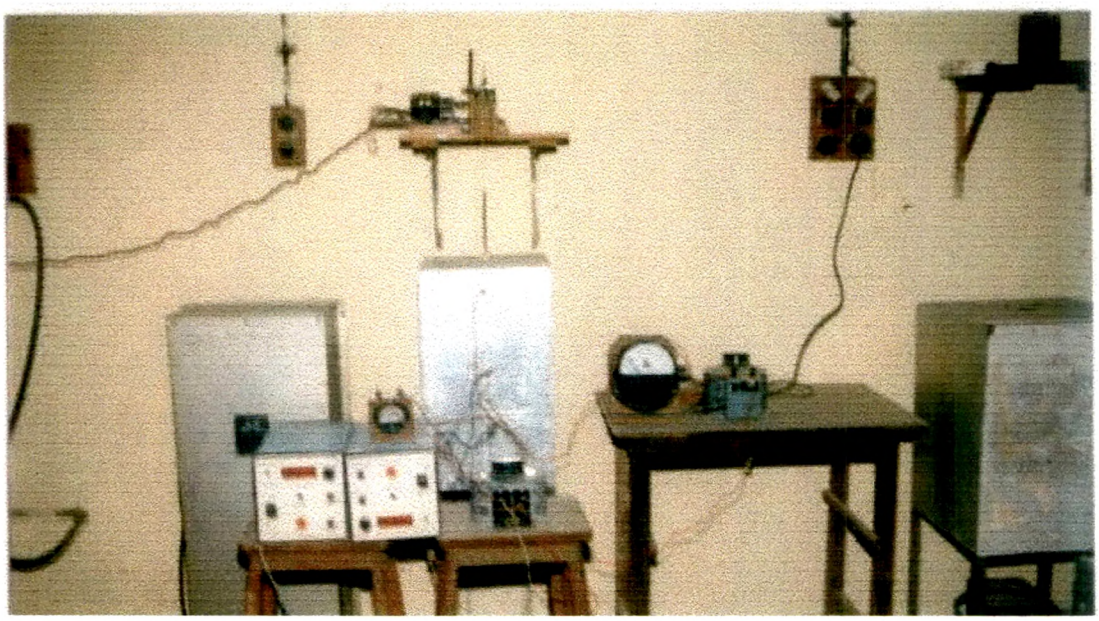

Fig. 5. Bridgman Furnace

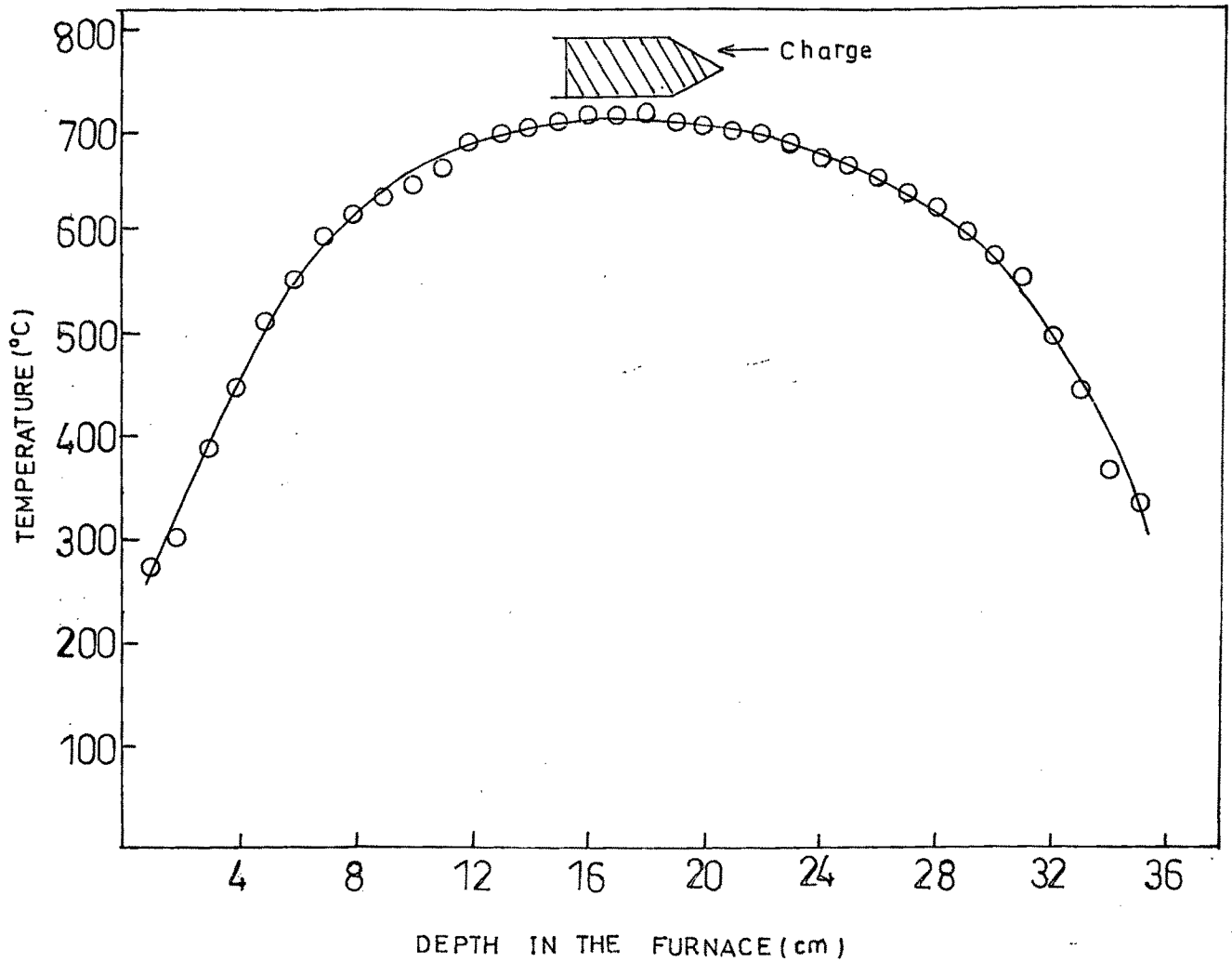

Fig. 6. Temperature Profile of the Bridgman Furnace

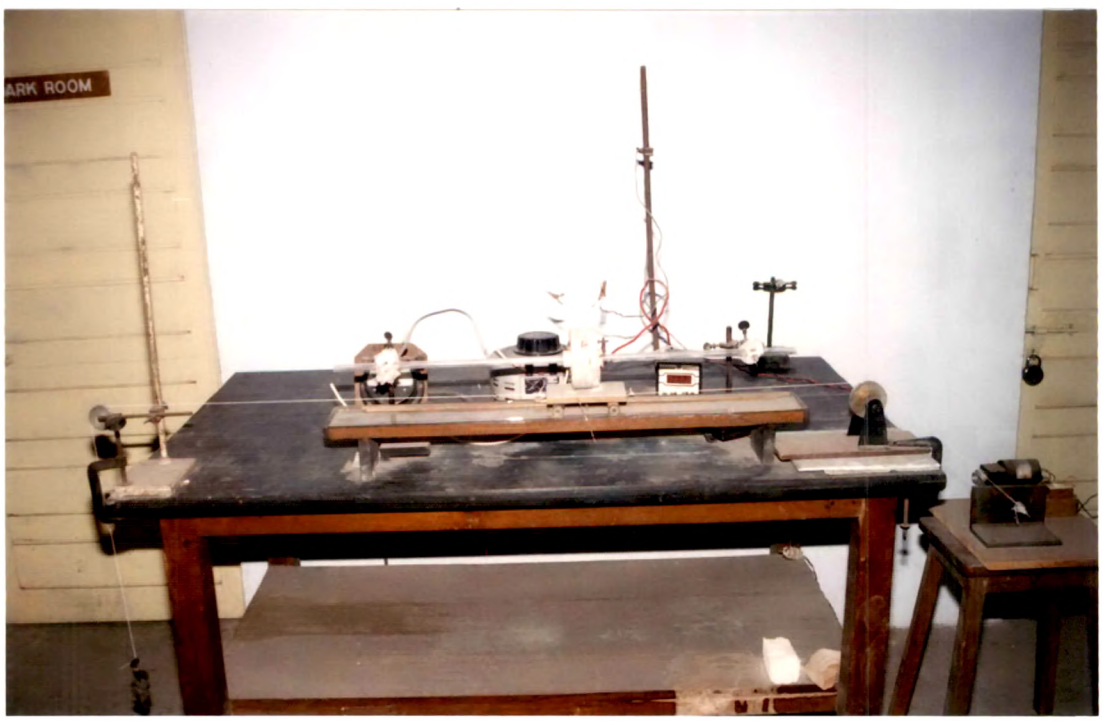

Fig. 7. Zone Melting Furnace

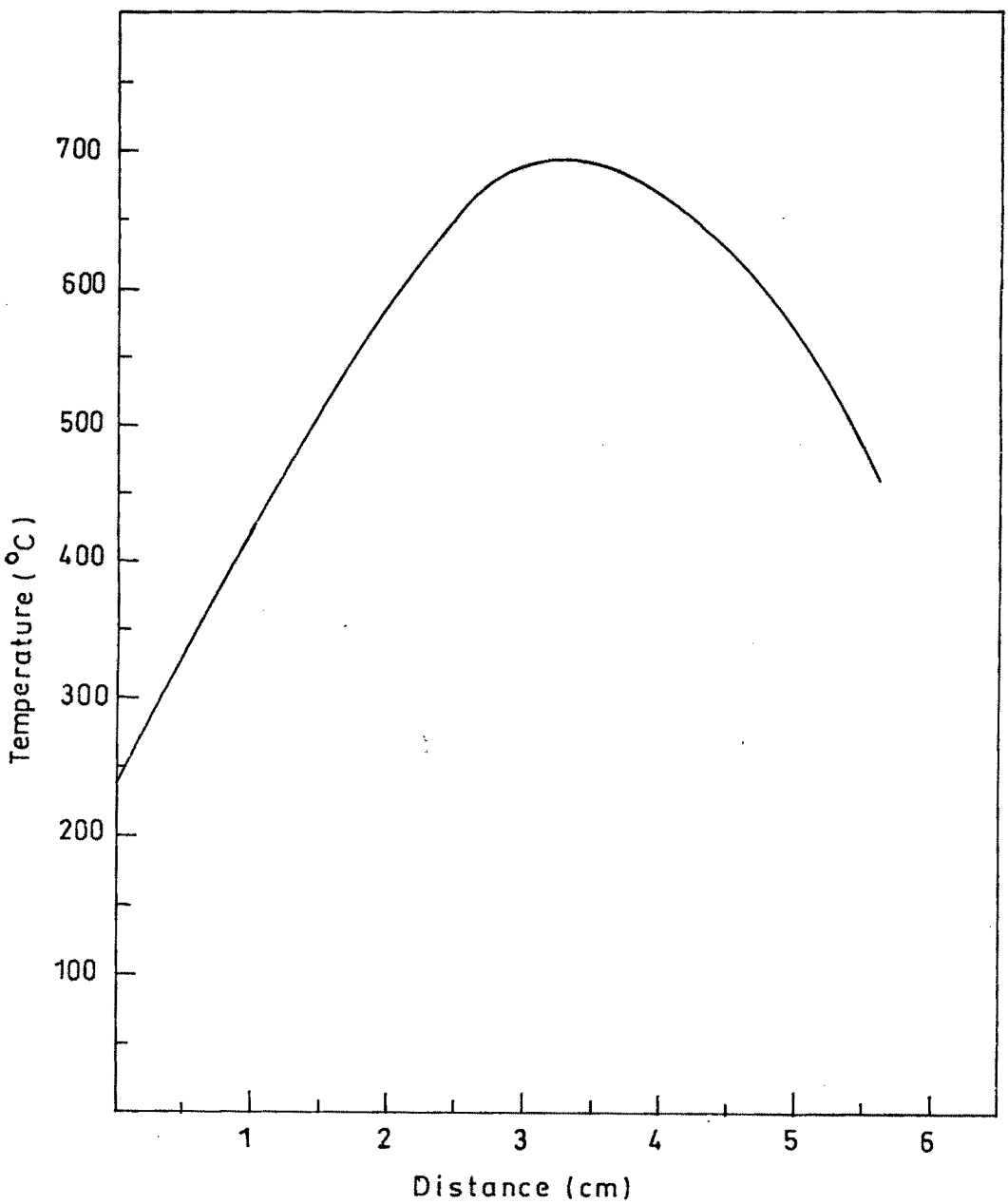

Fig. 8 Temperature Profile of Zone Melting Furnace

the last pass was used to obtain self-nucleated single crystals. The temperature gradient across the two solid-liquid interfaces was about 70°C/ cm giving a zone length of about 8 to 10 mm with maximum temperature of 700°C. The growth velocity was 0.35 cm/hr. To obtain good crystals it is necessary to give sufficient time to the first molten zone before starting the zone travel to achieve stable conditions.

CRYSTAL MORPHOLOGY

The term crystal morphology implies the study of crystal forms. However, in contrast to the old "physiography" of minerals, modern crystal morphology encompasses the external features as well as the internal structure of crystals, i.e. zones and pyramids of growth, cleavage cracks, inductive surfaces, corroded pits, etc. A knowledge of these details permits one to define more accurately the peculiarities in the formation of crystals, by reflecting the step-by-step history of their formation. However, these features occur only in natural crystals or crystals synthesized by a method which provides unconstrained free growth of crystals. It is known that the internal structure exerts a dominant influence during crystal formation. Because of this, the effect of external conditions on the crystal form is somewhat obscured. Surface morphology is not only an indicator of internal crystal perfection, but it also provides a link between this perfection and growth conditions.

In the preliminary stages of investigating a new system, characterization should begin with a microscopic examination. Hence in the present study of $Bi_xSb_{2-x}Te_3$ (x = 0, 0.2, 0.5, 1) and $In_{0.2}Sb_{1.8}Te_3$ crystals, for observation of crystal surfaces grown by Zone-melting and Bridgman technique, optical microscopy and occasionally electron microscopy has been used. Fig. 9 show the photograph of Vickers' projection microscope which was used for microtopographical study of the crystal surfaces. Vickers' projection microscope is an inverted metallurgical type microscope which also provides facilities for hardness testing, phase contrast and polarizing light microscopy as well as

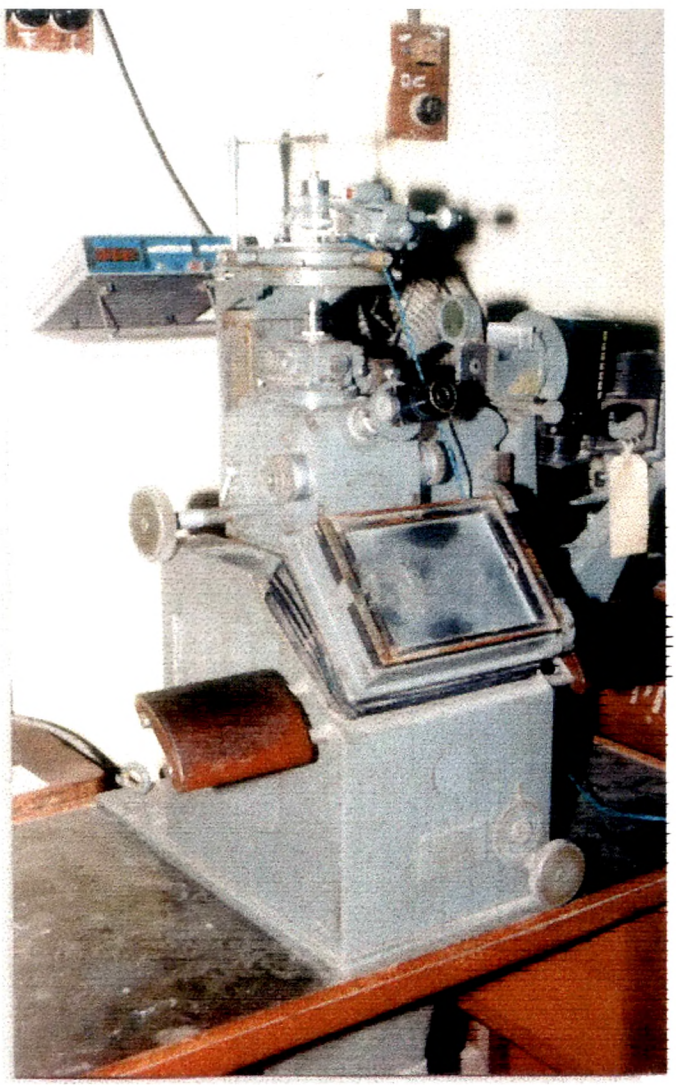

Fig. 9. Vicker's Projection Microscope

observation in transmission and reflection. Electron microscopy is a relatively advanced technique and superior to that of optical microscopy due to better resolution because of the shorter wavelength of electrons compared to light. In SEM the focussed spot produced by the electron source or gun is scanned across the specimen with a television type of raster by means of an electrostatic deflection system. Information about the specimen is obtained by detecting secondary electrons emitted from the specimen using a solid state detector. A photomultiplier signal is amplified and used to modulate the intensity of a synchronously scanned display tube to form a specimen image. The magnification is determined by the size of the display tube raster. Compared to the beam scan raster the typical range is 400 – 400,000X. Topographs are obtained in a matter of minutes with minimal sample preparation. However, it has to be noted that the entire operation is carried out in vacuum and use of very stable high voltage supply is important to ensure a constant wavelength.

Crystallographic features on the as-grown crystal surfaces of metals, semiconductors and their alloys have been observed by various workers[32-35]. These features arise often due to specific conditions involved in the crystal growth process. Mourizone et al.[36] observed features in the form of striations in InSb crystals. These striations were recognized as impurity striations. However, they have shown that the striations are related neither to the type and amount of impurity nor to the orientation and growth rate, but are rather dependent on the convection currents in the melt. Striations parallel to the growth axis have also been reported by Teghtsoonian and Chalmers[37] who associated the striations to the cellular structure of the solid-liquid interface. In the case of Bi-Sb alloy crystals, Bhatt et al.[38,39] observed striations on the free surface of the as-grown crystals as well as triangular and hexagonal crystallographic features on the cleavage plane. They have reported that these features are dependent on the growth rate and alloy composition and have shown that the striations are a result

of dendritic growth arising due to growth anisotropy which varies with alloy composition.

In the case of $Bi_xSb_{2-x}Te_3$ (x = 0, 0.2, 0.5, 1) and $In_{0.2}Sb_{1.8}Te_3$ crystals, no growth features have so far been reported. However, the present author has observed some interesting features on the as-grown single crystals and these are described below.

In the case of the $Bi_xSb_{2-x}Te_3$ (x = 0, 0.2, 0.5, 1) crystals grown by the Zone-melting technique, the top free surfaces of the as-grown crystals were found to exhibit well defined crystallographic features like rectilinear striations and symmetric close forms. In metals, alloys or intermetallic compound crystal growth, striations are not an unusual phenomena. No features were observed on the lower surfaces of the crystals, which were in contact with the quartz tube.

Fig. 10 shows a typical set of striations with inter-striation angle 120° observed in the case of $Bi_{0.2}Sb_{1.8}Te_3$ crystals. Fig. 11 shows similar striations but with a superimposed growth hillock which is of equilateral triangular shape. These two photographs above need be compared with Fig. 12 which shows a hexagonal growth step overlying a rhombus step. The angles in the geometry of these structures all were measured to be either 60° or 120° which correspond to the 3-fold symmetry pertinent to the crystal which belongs to the rhombohedral structure type. The directions of the edges and the planes involved in all these features therefore correspond to <111> and {111}, respectively. The phenomenon associated with these growth features should closely parallel the one observed and explained in the case of Bi-Sb alloy single crystals[39] in terms of advancing growth fronts. It has also been observed that, very frequently, triangular surface depressions [Fig. 13] resembling etch pits are attendant on the surfaces. These might have occurred due to a possible evaporation of the material from along preferential crystal planes, since two of the constituent elements, viz., Sb and Te, have relatively high vapour pressures.

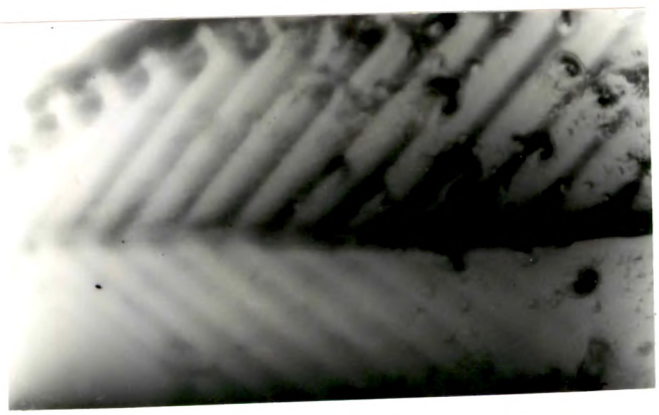

Fig. 10 X450

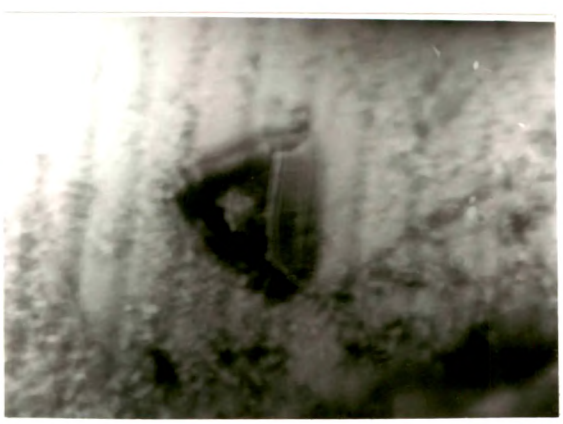

X450

Fig. 11

X 600

Fig. 12

X 800

Fig. 13

Fig. 14, 15 and 16 are SEM photographs of the growth features observed on the top free surface of the Sb_2Te_3 crystal grown by the zone-melting technique. Fig. 14 shows a region of bands containing ripples. The ripple formation is indicative of cellular growth arising from the constitutional supercooling. Fig. 15 and 16 show elevated growth hillocks on the surface. These might have occurred due to evaporation of Te from along the crystal surface and its recondensation.

There were also tiny whiskers frequently observed on the surface. These may be a result of the above mentioned hillocks surviving to grow further preferentially along one direction. H. Chung et al.[40] have reported simultaneous growth of CdTe and Te whiskers in the growth of CdTe crystals.

In the zone-melting method, larger surface area of the growing crystal is exposed. The crystal under study has a high vapour pressure constituent, viz., Te. Hence there are severe stoichiometric deviations expected. So this method of preparing Sb_2Te_3 and Sb_2Te_3-Bi_2Te_3 is considered unsatisfactory. Harman et al.[41] have also arrived at this conclusion in preparing Bi_2Te_3 by zone melting technique. They observed that much tellurium was lost through evaporation to the cooler portions of the tube and this results in ingots of varying compositions. They have proposed zone melting at high ambient temperature to prevent condensation of the volatile constituent which is present because of dissociation of the compound. However, compositional fluctuations are present in crystals grown by almost every other technique. One possible exception is the Bridgman technique where the vertical temperature gradients are stabilizing and, in the absence of vertically unstable density gradients of composition, there are no extensive growth transients. Thus to minimise the loss of the volatile constituents, the Bridgman method has been preferred for growing and studying properties of these crystals.

In the case of all the crystals grown by the Bridgman technique the side cylindrical surface was found practically free of any remarkable features except for occasional moderate cavities. Such cavities are observable in most of the Bridgman grown crystals e.g., Te[42]. Inside the cavity, features such as shown in

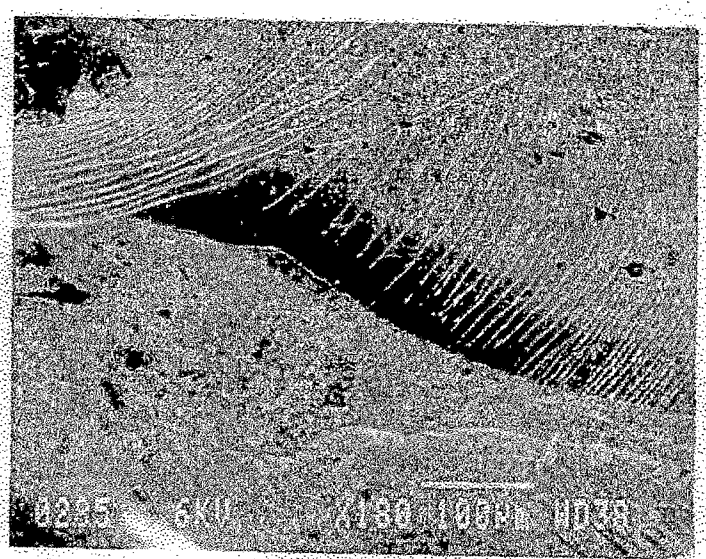

Fig. 14.

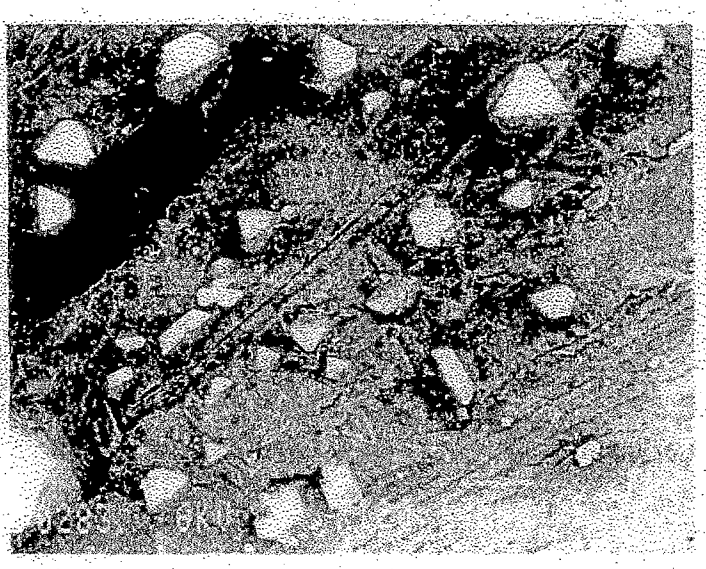

Fig. 15.

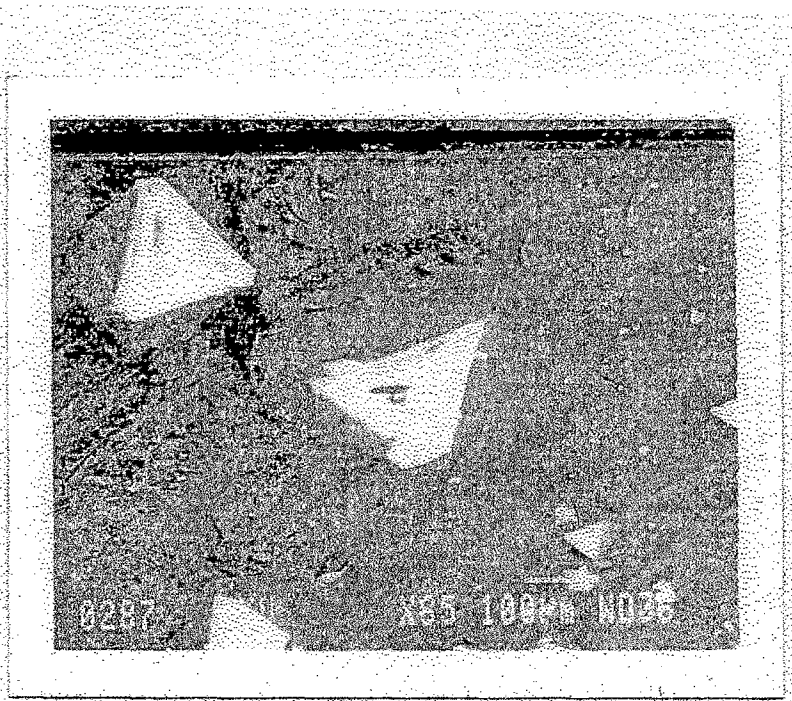

Fig. 16

Fig. 17 were observed. The planarity of the general surface and spreading layers indicate unconstrained growth progressing in the interior of the crystal away from the ampoule wall.

On the top free surface of the crystal, striated regions were observed accompanying the concave interface. The distribution of striations was found to define two regions on the surface : a central part and a peripheral part.

Fig. 18a shows the top view of the as-grown free surface of $BiSbTe_3$ crystal. Typically the crystal cleavage was easier in the central region than in the peripheral one. Fig. 18b is a photograph showing the peripheral region at a higher magnification. The curved striations observed in this region are actually continuations of the straight parallel striations observed in the central region. Growth striations also represent a chemical stress. They have been shown to be due to impurity segregation and, in a multicomponent system, to segregation of one of the components. Such transient segregations have been observed in Ga doped Ge pulled with crucible rotation only[43]. However, in the present case the striated morphology of the as-grown crystal surface can be assigned to transient thermal currents set up by temperature instabilities which are in turn usually caused by gradients, radial as well as longitudinal. The striations on a surface normal to the growth axis should then be specifically associated with the radial gradients. Ideally, there should not be any radial temperature gradient. Nevertheless, this cannot usually be eliminated because, apart from the furnace characteristics, the ampoule and material together produce such gradients owing to the vast difference in their thermal conductivities. Such features were observed in all the crystals grown by the Bridgman technique. To check whether these crystallographic surface features are restricted to the surface or occur as a result of body phenomena, the samples of Bridgman grown crystals were cleaved and the surfaces were observed under microscope. It was found that the cleavage plane was almost parallel to the growth axis. Except for few cleavage lines, which may

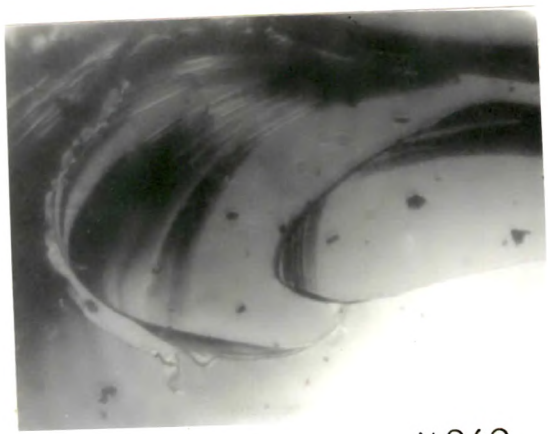

X 340

Fig. 17

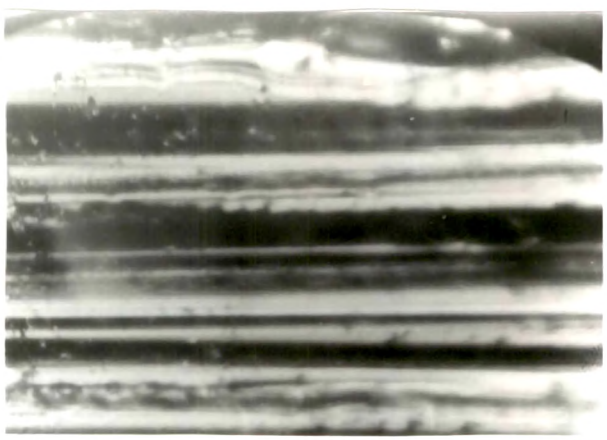

X 340

Fig. 18 a

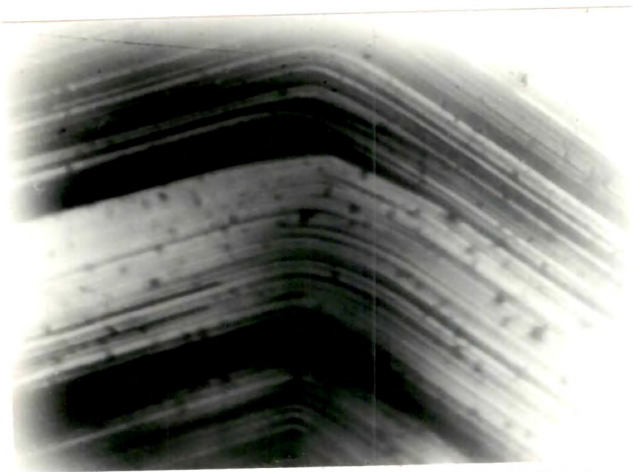

X 340

Fig. 18 b

be due to the stress introduced during the act of cleaving, the planes were seen to be free of any structures which may resemble striations.

The top region of the crystals grown by the Bridgman technique was in general concave shaped with ridging resulting into complex cross-section. Hence this portion of the crystal was discarded for further investigations. The crystals were cut, lapped and polished for thermoelectric measurements (the details are given in Chapter 9). Although the surface was observed to be plane and mirror like, there were frequent microcavities observed which might have been a result of occluded gases. The gas inclusion is usually unavoidable except if some elaborate high temperature high vacuum degassing treatment is given to the material before the growth process.

The crystals grown by the Bridgman technique were used for further characterization study as discussed in next chapters.

CONCLUSION

1) In the case of crystals grown by the zone melting technique, the observations of the growth features indicates cellular growth mechanism due to constitutional supercooling to be effective in the growth of the crystals and stoichiometric deviation of the material due to preferential evaporation of tellurium.

2) Single crystals of $Bi_xSb_{2-x}Te_3$ (x= 0, 0.2, 0.5, 1) and $In_{0.2}Sb_{1.8}Te_3$ have been obtained by the Bridgman technique at the rate of 0.35 cm/h under a gradient of 35°C/cm . The existence of microcavities due to gas inclusions are unavoidable which might have serious effects on thermoelectric measurements.

REFERENCE

[1] Abrikosov, N. Kh., Ivanova, L. D. and Aladashvili, N. S. (1979) Izv. Akad. Nauk SSSR, Neorg. Mater. 5, 1766.

[2] Abrikosov, N. Kh. and Ivanova, L. D. (1982) Izv. Akad. Nauk SSSR, Neorg. Mater. 18, 560.

[3] Berkholtz, U. (1958) Z. Naturforsch. 13a, 780.

[4] Testardi, L. R. and Wiese, J. R. (1961) Trans. Met. Soc. AIME 221, 647.

[5] Cosgrove, G. J., McHugh, J. P. and Tiller, W. A. (1961) J. Appl. Phys. 32, 621.

[6] Wiese, J. R. and Pyle, Richard (1960) J. Metals 12, 715.

[7] Rosi, F. D., Abeles, B. and Jengen, R. V. (1959) J. Phys. Chem. Solids 10, 191.

[8] Yasuda, H., Ohnaka, I., Furukubo, Y., Fukuda, T., Watanabe, K. and Koh, H. J. (1998) J. of the Japan Institute of Metals 61 (12) 1288.

[9] Koenig, F. (1998) Cryst. Res. Technol. 33 (2) 219.

[10] Ivanova, L. D., Brovikova, S. A., Sussmann, H. and Reinshaus, P. (1994) Inorg. Mater. 30, 716.

[11] Ivanova, L. D., Brovikova, S. A., Sussmann, H. and Reinshaus, P. (1994) Inorg. Mater. 30, 48.

[12] Ivanova, L. D., Brovikova, S. A., Sussmann, H. and Reinshaus, P. (1995) Inorg. Mater. 31, 682.

[13] Fleurial, J. P., Gaillard, L., Triboulet, R., Scherrer, H. and Scherrer, S. (1988) J. Phys. Chem. Solids, 49, 1237.

[14] Gailliard, L., Caillat, T., Scherrer, H. and Scherrer, S. (1989) 8th International Conference on Thermoelectricity (ICT), Nancy, Edited by H. Scherrer, and S. Scherrer.

[15] Caillat, T., Carle, M., Pierrat, P., Scherrer, H. and Scherrer, S. (1992) J. Phys. Chem. Solids 53, 1121.

[16] Rosenberg, A. J. and Strauss, A. J. (1961) J. Phys. Chem. Solids 19, 105.

[17] Yim, W. M. and Rosi, F. D. (1972) Solid State Electronics 15, 1121.

[18] Durst, T., Goldsmid, H. J. and Harris, L. B. (1981) Solar Energy Materials 5, 181.

[19] Kaibe, H. Tanaka, Y., Sakata, M. and Nishida, I. (1989) J. Phys. Chem. Solids 50, 945.

[20] Kagawa, S., Satake, H., Sakamoto, M., Yamamoto, A. and Ohta, T. (1997) Proc. 16th International Conference on Thermoelectrics (ICT), Dresden, Germany, 85.

[21] Seo, J. H., Lee, D. M., Park, K. and Lee, C. H. (1997) Proc. 16th International Conference on Thermoelectrics (ICT), Dresden, Germany, 81.

[22] Amin, F. A. A., Al-Ghaffari, A. S. S., Issa, M. A. A. and Hassib, A. M. (1992) J. Mater. Sci. 27, 1250.

[23] Goldsmid, H. J. and Penn. A. (1986) Phys. Lett. 27A, 523.

[24] Hann, S. H., Gshneidner Jr., K. A. and Beaudry, B. J. (1992) J. Alloys and Compounds 181, 463.

[25] Ohta, T., Yamamoto, A. and Tanaka, T. (1995) AIP (American Institute of Physics) Conf. Proc. 267.

[26] Pfann W. G. (1952) Trans. AIME 194, 747.

[27] Bridgman, P. W. (1925) Proc. Am. Acad. Arts and Sci., 60, 303.

[28] Poretskaya, L. V., Abrikosov, N. Kh. And Glazov, V. M. (1963) Zh. Neorg. Khim., 8, 1196.

[29] Smith, M. J., Knight, R. J. and Spencer, C. W. (1962) J. Appl. Phys. 33, 2186.

[30] Hansen, M. and Anderko, K. (1958) Constitution of Binary Alloys, 2nd ed., McGrawHill, New York.

[31] Offergeld, G. and Cakenberghe, J. (1959) J. Phys. Chem. Solids 11, 310.

[32] Stewart, M. T., Thomas, R., Wauchope, K., Winegard, W. C. and Chalmers, B. (1951) Phys. Rev. 83, 657.

[33] Ueda, H. J. (1961) J. Phys. Soc. Jap. 16, 61.

[34] Camp, P. R. (1954) J. Appl. Phys. 25, 459.

[35] Gatos, H. C., Strauss, A. J., Lavine, M. C. and Harmon, T. C. (1961) J. Appl. Phys. 32, 2057.

[36] Mourizone, K., Witt, A. F. and Gatos, H. C. (1966) J. Electrochem. Soc. 113, 51.

[37] Teghtsoonian, E. and Chalmers, B. (1951) Can. J. Phys., 29, 370.

[38] Bhatt, V. P., Rao, R. D., Pandya, G. R. and Vyas, A. R. (1976) Ind. J. Pure and Appl. Phys. 14, 537.

[39] Pandya, N. S., Bhatt, V. P., Pandya, G. R. and Rao, R. D. (1977) Ind. J. Pure and Appl. Phys. 15, 444.

[40] Chung, H., Chea, Y. and Kim, K. B. (1968) J. Korean Phys. Soc., 1, 112.

[41] Harman, T. C., Paris, B., Miller, S. E. and Goering, H. L. (1957) J. Phys. Chem. Solids 2, 181.

[42] Trivedi, M. D. (1977) Ph.D. Thesis, M. S. Univ. of Baroda, Vadodara, India, 50.

[43] Carruthers, J. R. and Witt, A. F. (1974) Crystal Growth and Characterization (Proc. Of ISSCG2 Spring School, Japan) Editors, R. Ueda and J. B. Mullin, North Holland Publishing Company, Amsterdam, p.142